Why dissolved organics matter: DOC in ancient oceans and past climate change

ANDY RIDGWELL [1]
SANDRA ARNDT [1]

[1] *School of Geographical Sciences, University of Bristol, Bristol (UK)*

Corresponding author*:*
Andy Ridgwell
School of Geographical Sciences
University of Bristol
University Road
Bristol BS8 1SS
UK
Tel: +44 (0)117 928 9954
Fax: +44 (0)117 928 7878
Email: andy@seao2.org

To be submitted to:
Manuscript date: **April 16, 2014**

Table of Contents

1. Overview

The ocean and its underlying sediments are the largest sinks of CO_2 within the Earth system that are able to respond to changes in atmospheric CO_2 on both human induced (anthropogenic) and geologically relevant time scales. We need a complete understanding of their dynamics and strength of feedbacks with climate and other drivers of global change if we are to make confident projections regarding the full consequences of continued fossil fuel CO_2 emissions. To this end, in the past couple of decades we have made rapid progress in elucidating the roles that basic physical (e.g., ocean circulation) and inorganic geochemical processes (e.g., gas exchange) play in regulating the uptake of CO_2 from the atmosphere. In contrast, the role and response of the 'biological carbon pump' – the interplay of biological, geochemical and physical processes that transfer carbon from the surface ocean where it is fixed by primary producers, to depth where it is either consumed or buried in the underlying sediments – is much less well understood. Even the sign of some of the main feedbacks involved and whether the response of the biological carbon pump will act to amplify or reduce future climate warming and ocean de-oxygenation is somewhat uncertain.

Two research directions are providing new insights into the marine carbon cycle and how it responds to perturbation. The first revolves around on-going efforts to understand the mechanistic operation of the biological carbon pump and in particular the cycling of carbon through dissolved organic carbon (DOC) in the ocean, as described in this book. The second is an increased appreciation of what might be learned from the geological record. Earth history is punctuated by a huge variety of transitions and perturbations in climate and global biogeochemical cycles, with some events exhibiting evidence for greenhouse warming and CO_2 release and hence potentially providing clues regarding future changes. The conjunction of these two developments has led to the idea that both the cycling of carbon through DOC and its reservoir size could have been fundamentally different in the past, and that change in that cycling may be mechanistically linked to major events in the geological record. The

69 breath of speculation about how the marine carbon cycle may have operated during the Precambrian
70 (prior to 541 Ma) and under very different conditions of oxygenation and ecosystem function from
71 today, also highlights the importance of first being able to ground our geologic interpretation in a full
72 mechanistic understanding of the sources and sinks of DOC in the modern ocean.

73 This chapter provides an overview of how the proposed link between DOC and major global
74 carbon cycle perturbations in the geological record arises. We start by presenting a brief summary of
75 how the marine carbon cycle operates. We then introduce how the geological record can be interpreted,
76 focusing on the ways in which the carbon isotopic signature of sedimentary rocks reflects past changes
77 in global carbon cycling. We finish by critically assessing recent thinking regarding the potential role
78 of DOC dynamics as a driver or amplifier of extreme climate events in the past as well as the potential
79 future implications.

80

2. Marine carbon cycling

Geological rock reservoirs dominate the global inventory of carbon on Earth (Figure 1). However, the response time for the formation or any substantive depletion of these reservoirs is counted in 10s, if not 100s, of millions of years, being largely governed by plate tectonics and major biological evolutionary innovations such as the advent and proliferation of calcifying plankton [*Ridgwell*, 2005]. At ~38000 PgC (1 PgC = 10^{15} gC), the present-day ocean dissolved inorganic carbon (DIC) reservoir is the next largest carbon store on Earth and is an order of magnitude larger than the likely extractable resources of fossil fuel carbon or the terrestrial biosphere (and soils). One way to influence atmospheric pCO_2 and climate via greenhouse warming is to create an imbalance in the inputs versus sinks of carbon to the ocean. However, the response time of the ocean plus atmosphere as a whole – calculated as its carbon inventory (Figure 1) divided by the rate of carbon throughput from weathering and mantle CO_2 out-gassing (Figure 2b,c), comes out to be of the order of 100 thousand years (100 kyr). Perturbations of the global carbon cycle that change the DIC inventory of the ocean as a whole in this way are hence only arguably relevant on geological time-scales. Ocean alkalinity (and *p*H) influences the speciation of DIC speciation (between $CO_{2(aq)}$, HCO_3^-, and CO_3^{2-}), but similar time-scales apply if one wishes to changes the alkalinity inventory of the ocean as a whole.

Dissolved inorganic carbon (and alkalinity) can also be partitioned spatially within the ocean. This is important as the atmosphere only 'sees' the surface ocean. The rapid exchange of CO_2 between ocean surface and atmosphere (Figure 2a) means that atmospheric pCO_2 and hence climate are highly responsive to changes in surface DIC which gives the ocean a unique importance to the global carbon cycle and climate system for reasons beyond its relative total carbon mass.

2.1. A tale of three ocean carbon 'pumps'

A variety of biogeochemical processes act to segregate carbon against the homogenization tendencies of physical mixing and ocean circulation. For convenience, how the partitioning of DIC between the surface ocean and ocean interior as well as its speciation at the surface are controlled, is traditionally divided into three conceptual 'pumps' in the ocean (e.g. *Sarmiento and Gruber* [2006]): (1) the 'solubility' pump, (2) the 'organic matter' ('organic carbon' or 'soft tissue') pump, and (3) the 'carbonate' (or 'counter') pump, illustrated in Figure 2. In this conceptual framework, all three oceanic carbon pumps act primarily by vertically re-locating carbon away from the surface, hence the concept of the 'pumping' of carbon from the surface to depth. At the same time, the latter two also partition alkalinity (ALK) (see *Stumm and Morgan* [1981] or *Zeebe and Wolf-Gladrow* [2001] for details) with depth, thus dictating the speciation of DIC (the balance between $CO_{2(aq)}$, HCO_3^-, CO_3^{2-}) to maintain overall charge neutrality. Modulating all three and hence influencing atmospheric pCO_2 are the large-scale patterns and rates of ocean circulation that control the return of DIC, ALK, and nutrients back to the surface.

The operation of the solubility pump in partitioning DIC between surface and the deep ocean is the simplest to conceptualize (Figure 2a). CO_2 is more soluble in colder compared to warmer seawater. As a consequence, carbon dissolution is enhanced in cold, high latitude surface waters, where deep waters form. The rapid sinking of these dense, DIC-rich surface waters and their re-distribution in the deep ocean results in an efficient pumping of carbon from the atmosphere to the deep ocean. Apart from temperature, the solubility of CO_2 is also affected by salinity. Thus, differences in salinity between major water masses and between surface and deep ocean will also make a contribution. Nevertheless, the contribution of salinity is generally minor compared to the effect of temperature.

The 'organic matter' ('organic carbon' or 'soft tissue') pump also acts to induce a vertical DIC gradient (Figure 2b). In this case, DIC is removed from solution as a result of photosynthesis and its fixation in the form of both particulate organic carbon (POC) and DOC. A proportion of POC escapes

127 the intense recycling in the surface ocean, sinking vertically through the ocean interior, where
128 heterotrophic degradation results in its remineralization to DIC. In general, the heterotrophic
129 degradation of POC during sinking is highly efficient, with <1-6% of the POC export production
130 reaching the seafloor, where of this flux, just 0.3% escape benthic degradation to be buried [*Dunne et*
131 *al.*, 2007]. The further the POC sinks before the associated carbon is released back to the DIC pool, the
132 more effective the partitioning between surface and deep ocean. Any reduction (or increase) in the
133 efficiency of this degradation during sinking, perhaps as a result of changes in sinking speed or
134 microbial degradation rate, thus has the potential to affect pCO_2. The influence of the organic carbon
135 pump is partially offset by alkalinity changes associated with nitrogen transformations, particularly
136 from NO_3^- to organic N during photosynthesis and from organic N to NH_4^+ during heterotrophic
137 degradation [*Zeebe and Wolf-Gladrow*, 2001] which at the surface has the effect of partitioning more
138 DIC in the form of $CO_{2(aq)}$. In addition, the organic carbon pump controls nutrient cycling in the ocean:
139 creating nutrient-rich deep waters that are re-distributed by global circulation and upwelling and
140 thereby influencing the spatial distribution of primary production in the ocean.

141 The third of the traditional carbon pumps, the carbonate pump, involves the biological
142 precipitation of calcium (and to a lesser extent, magnesium) carbonate ($CaCO_3$) at the ocean surface.
143 Perhaps as much as 50% of carbonate dissolves as it sinks [*Feely et al.*, 2004]. The remainder reaches
144 the sediment surface where ~20% of the deposited carbonate escapes further dissolution to be buried
145 [*Feely et al.*, 2004], ultimately forming a new geological carbon reservoir (Figure 2c). Although the
146 carbonate pump also vertically redistributes carbon, the transfer of alkalinity dominates in terms of its
147 influence on the speciation of dissolved carbon species and hence it acts to increase, not decrease,
148 surface ocean fCO_2.

149 By virtual of the their influence on surface ocean [$CO_{2(aq)}$], all three of the pumps play an
150 important role in the short-term carbon cycle. We define 'short term' here as the approximate mixing

time scale of the ocean (nominally ~500-1000 years). This choice of time scale ensures that the geochemical redistribution initially arising from any transient change in any of the C pumps will have been effectively homogenized by ocean mixing beyond a couple of mixing cycles. On short time scales, the organic carbon pump dominates over the carbonate pump in terms of net influence on atmospheric pCO_2, simply as a result of its order-of-magnitude larger export flux. The organic matter pump also dominates over the solubility pump [*Cameron et al.*, 2005].

All three pumps are also important components of the long-term carbon cycle, driving the accumulation, biogeochemical transformation, and burial of carbon in marine sediments; directly in the example of the two solid pumps and indirectly in controlling the saturation state and oxygenation of bottom water in the case of the solubility pump. For instance, under conditions conducive to the preservation of biogenic calcium carbonate ($CaCO_3$) – primarily the shells of haptophyte algae (coccolithophores) and zooplankton (foraminifera) – sediments can become rich in $CaCO_3$, with large amounts of carbon locked away for millions of years in the form of chalk deposits. As mentioned earlier, the sediment preservation of organic matter is generally less efficient, with only a tiny fraction of the organic matter that is exported from the surface ocean ultimately buried. Nevertheless, organic carbon burial rates can vary significantly in space and time. Particular intervals of Earth history, for instance, the Cretaceous (145.5 and 65.5 Myrs ago (Ma)) and Jurassic (201.3 to 145.5 Ma) saw a widespread deposition of organic carbon rich (>1 wt%) strata. The factors that may explain this spatial and temporal variability in organic carbon deposition and burial rates are a matter of debate. They include, but are not limited to, organic matter composition, terminal electron acceptor and in particular oxygen availability, benthic community composition, microbial inhibition by specific metabolites, priming, physical protection, deposition rate and macrobenthic activity (see review by *Arndt et al.* [2013]). In addition, the enhanced deposition and burial of organic matter may promote the production of methane (CH_4) in the anoxic sub-seafloor. In conjunction with cold temperatures and/or high

pressure, hydrates can form – molecules of CH_4 trapped in a water ice cage structure [*Maslin et al.*, 2010]. Methane hydrates are special amongst the geological reservoirs in that they also influence the global carbon cycle and climate on short time scales if the environmental conditions change sufficiently rapidly and substantially to destabilize the hydrate structure and release the CH_4 gas. An increase in ocean temperatures and depressurization by slumping and loss of the overlying sediment burden are possible drivers of significant CH_4 release (e.g. see *Maslin et al.* [2010]).

The last glacial maximum (LGM; about 21 thousand years ago) is a good example of the role that the ocean carbon pumps play in regulating atmospheric pCO_2. At the time of the LGM, the concentration of CO_2 in the atmosphere was about 190 ppm compared to ~260 ppm at the start of the Holocene (11700 years ago) and ~280 ppm just prior to the industrial revolution (nominally year 1765) [*Monnin et al.*, 2001]. An enduring mystery is 'why'? Or in other words, in what way did the global carbon cycle function differently, resulting in lower atmospheric CO_2 during glacial periods [*Kohfeld and Ridgwell*, 2009]? Aside from ideas about lower glacial ocean temperatures and hence an increase in the strength of the solubility pump, a greater supply of aeolian iron to surface ocean ecosystems and hence partial relief of iron limitation in regions such as the Southern Ocean may have played a role [*Watson et al.*, 2000]. Iron deposition works its magic on atmospheric CO_2 via an increase in plankton productivity and POC export and hence a stronger organic matter pump in the ocean – increasing the partitioning of DIC away from the surface and to depth. The biological pump could have been more 'efficient' as well as stronger – an important distinction to make. In terms of lowering atmospheric pCO_2 – it is not sufficient to simply export POC away from the surface more rapidly through increased biological export; the CO_2 that is eventually released through biological remineralization needs to be kept away from the ocean surface and hence the atmosphere for as long as possible. For instance, carbon released from the degradation of POC in a more stratified glacial deep ocean [*Atkins et al.*, 2002] would be less effectively mixed back towards the surface, whilst colder ocean temperatures

199 could potentially have reduced the degradation rate of settling POC (e.g. *Jørgensen and Sørensen*,
200 [1985], *Crill and Martens*, [1987]; *Matsumoto et al.* [2007]) and pushed the average depth at which
201 DIC is released to greater depths. Both processes would act to increase the efficiency of the biological
202 carbon pump, even if a side-effect was decreased export from the surface due to reduced nutrient
203 return. That the question has yet to be settled, despite the existence of a wide variety of hypotheses
204 [*Kohfeld and Ridgwell*, 2009], points to a still incomplete understanding of the marine carbon cycle and
205 leaves the potential for new mechanisms and processes to be discovered.

206 *2.2. A fourth appears – the microbial carbon pump*

207 Appreciation of the 'microbial carbon' pump (Figure 2d) – a part of the biological pump involving the
208 net production of DOC by microbial processing of organic matter, has increased rapidly over the past
209 decade [*Jiao et al.*, 2011]. It represents a further mechanism for re-partitioning carbon amongst the non
210 geological (surficial) reservoirs. Alongside the production of POC and PIC by marine phytoplankton at
211 the surface ocean, a variable but substantial fraction of primary production (30-50%) is released as
212 DOC (e.g., *Ducklow et al.* [1995]; *Biddanda and Benner* [1997]). DOC is also created by a variety of
213 other activities in the surface ocean, including viral lysis, 'sloppy feeding' by metazoan grazers, the
214 egesta of protists and metazoa [e.g. *Jiao et al.* 2010] and the initial extracellular hydrolysis step
215 involved in heterotrophic POC degradation. The most labile fractions of DOC are consumed rapidly
216 and account for a mere 1% of the total ocean DOC inventory [*Hansell*, 2013]. Only the more
217 biologically recalcitrant DOC fractions last long enough to be transported into the deep ocean by ocean
218 circulation. Even so, few of these newly produced, recalcitrant DOC fractions survive to reach depths
219 of 1000 m [*Hansell*, 2013]. The mineralization product (DIC) will still continue to be advected into the
220 ocean interior however; helping partition DIC into the ocean interior.

221 In contrast, at the highly refractory end of the reactivity spectrum, refractory DOC (RDOC) is
222 removed only on multi-millennial time scales and hence on average survives multiple cycles of ocean

223 turnover. Presumably, direct exudation during bacterial production, viral lysis of microorganisms or
224 microbial necromass further contribute to the refractory pool. Microbial activity thus transfers, by the
225 successive processing of DOC, organic carbon from low concentrations of reactive carbon to
226 progressively higher concentrations of refractory carbon (hence the 'pump' designation; *Jiao et al.*
227 [2010]). Despite its relatively low rate of production – perhaps only 0.043 PgC yr^{-1} [*Hansell*, 2013] as
228 compared to 1-10 PgC yr^{-1} for PIC and POC export (Figure 1), the most refractory DOC component
229 accumulates in the ocean with estimated inventories of 630± 12 PgC for RDOC and >12 PgC for an
230 ultra-refractory (e.g., black carbon) DOC [*Hansell*, 2013]. As such, RDOC constitutes a reservoir of
231 similar size to the atmospheric burden of carbon present as CO_2 (Figure 1). Thus, although the
232 existence of this refractory carbon pool has been known for decades (e.g. *Hedges* [2002]), its potential
233 size and thus its potential significance for carbon sequestration and past and potentially also future
234 climate change, has only been recognized recently (e.g. *Jiao et al.* [2010]).

235 In theory, any substantial change in the consumption (or mineralization) rate of this DOC pool
236 could exert a large effect on atmospheric pCO_2 and climate. A variety of environmental factors such as
237 oxygen availability and ecosystem or temperature changes could potentially trigger substantial changes
238 (see several other chapters in this book for insights on the processes that control the composition,
239 reactivity, production and removal of DOC in the ocean). In particular, the availability of oxygen often
240 plays a central role in the discussion of substantial and large scale changes in organic carbon
241 consumption rates on climate relevant time scales. Although the jury is still out on the direct effect of
242 oxygen availability on heterotrophic organic carbon degradation, preservation of organic carbon tends
243 to increase under anoxic conditions (e.g. *Canfield et al.* [1993]). This increase could be the result of a
244 thermodynamically limited degradation of refractory organic compounds in the absence of the powerful
245 electron acceptor oxygen, the inability of anaerobic organisms to directly and completely degrade
246 organic matter to CO_2, a decreased enzymatic activity and/or a decreased availability of DOC adsorbed

247 to mineral surfaces under anoxic conditions (e.g. see review by *Arndt et al.* [2013]). Therefore, large
248 scale ocean redox changes could, in theory, result in a larger global ocean DOC inventory during
249 periods of widespread ocean anoxia. This pool of DOC would then be rapidly oxidized to DIC once
250 oxic conditions are re-established, releasing large amounts of carbon into the ocean-atmosphere system.
251 This hence provides a new mechanism to alter the DIC inventory of the whole ocean and one that can
252 operate with a response time much faster than the ~100 kyr time-scale driven by imbalances between
253 weathering on land and sediment burial at the ocean floor. The possibility that such situations occurred
254 in the geological past is the subject of the remainder of this chapter.

255

256 ## 3. Interpreting the geological past

257 A plethora of biological, geochemical and physical factors, such as ecosystem composition, the
258 reactivity and fate of organic matter, oxygen levels of the ocean's interior, and the cycling of nutrients,
259 together control the strength and efficiency of the biological pump [*Hain et al.*, in press]. These factors
260 interact with and respond to changes in climate. The resulting complexity makes it extremely
261 challenging to make projections about the consequences of continuing global warming on the marine
262 carbon cycle. The geological record helps here as Earth history is punctuated by a huge variety of
263 transitions and perturbations in global biogeochemical cycles and climate. These perturbations may
264 exhibit evidence for greenhouse warming and CO_2 release [*Hönisch et al.*, 2012], with some associated
265 with major extinctions or biotic disruption. Such events potentially provide calibrations regarding, for
266 instance, the response of marine ecosystems to ongoing global change (e.g. *Gibbs et al.* [2006, 2012]),
267 for which model-based projections are difficult.

268 ### *3.1. Carbon isotopes as proxies for past global carbon cycle changes*

269 To understand past carbon cycle feedbacks and biotic sensitivities, we need to know how
270 environmental conditions have changed and the relationship between them, such as between
271 atmospheric CO_2 concentration, surface temperatures [*Dunkley Jones et al.*, 2013], ocean *p*H and
272 carbonate saturation [*Hönisch et al.*, 2012], or depletion of the ocean's oxygen inventory [*Keeling* et
273 al., 2010]. However, reconstructing environmental variables is an imperfect science that becomes
274 increasingly difficult as one goes further back in time. To about 800 kyr ago (800 ka), ice cores drilled
275 from the Antarctic ice cap reveal the composition of the ancient atmosphere (including, critically,
276 pCO_2) encoded in bubbles [*Lorius* et al., 1993; *Etheridge* et al., 1996]. Additional environmental
277 variables, such as the fluxes of dust and aerosols to the ice sheet surface, are recorded as impurities in

278 the ice itself [*Lambert* et al., 2012]. Beyond this, we have no direct record of the concentration of CO_2
279 in the atmosphere and therefore have to rely on geological 'proxies'.

280 Proxies (here, entities or measures representing the value of something else) are rooted in
281 measurements made of some physical property in a geological sample such as, for instance, the mass
282 fraction of a particular solid component (e.g., $CaCO_3$) or a geochemical property, such as the ratio
283 between different trace elements or isotopes of the same element [*Wefer* et al., 1999]. The intent with
284 proxies is to empirically (or in rare cases, theoretically) calibrate a physical or geochemical property
285 against an environmental variable of interest. Such calibrations are based on a combination of
286 laboratory manipulation experiments and correlations inherent in modern observations. For instance,
287 the density of stomata – the physiologically controlled pores in the underside of leaves that regulate
288 both CO_2 ingress and water vapor loss – tends to decrease with increasing ambient pCO_2 [*Royer,* 2001].
289 The reason is that while plants require CO_2, they equally need to conserve water. Higher atmospheric
290 pCO_2 simply means that fewer stomata are required by the plant in order to obtain the same diffusive
291 flux of CO_2. Fewer stomata provide the benefit of reduced water loss. Hence, the density of stomata,
292 which can be counted in fossil leaves, should track the concentration of CO_2 in the atmosphere if the
293 plant requires that water loss be minimized. However, for many environmental variables no direct
294 proxy may exist. Therefore, reconstruction of potential past environmental conditions and the testing of
295 hypotheses relies on more indirect proxies. The ratio of the stable isotopes of carbon recorded in
296 sedimentary rocks has been particularly important in this respect and has been central to efforts in
297 reconstructing past global carbon cycling.

298 Carbon has two stable isotopes with masses 12 and 13 and a mean global ratio of ~89:1. By
299 convention, the 12:13 ratio in a sample is written in the delta-notation:

300 $$\delta^{13}C_{\text{sample}} = (R_{\text{sample}} / R_{\text{standard}} - 1) \times 1000 \quad (1)$$

where R_{sample} is the $^{13}C/^{12}C$ ratio measured in the sample and R_{sample} is the $^{13}C/^{12}C$ ratio in a substance of known composition (a standard). The sample isotopic composition ($\delta^{13}C_{sample}$) is scaled by a factor of 1000 and given in units of per mil (‰).

Isotope fractionation – a change in the ratio of 12:13 during conversion of one carbon-containing substance to a second – can occur under a number of circumstances (see Beaupré chapter). First, at the same temperature and hence same kinetic energy, the lighter isotope (^{12}C) has a higher velocity. During diffusion, the destination will become isotopically depleted (in ^{13}C) while the source of carbon will become enriched. Second, covalent bonds involving ^{13}C are stronger than those involving ^{12}C. Hence, the photosynthetic splitting of CO_2 and the breaking of bonds in organic molecules tends to occur to a greater extent for ^{12}C, again leaving the residual enriched in ^{13}C. The result of kinetic and particularly bond-breaking fractionation, as carbon moves between different carbon reservoirs and is transformed, is that the carbon reservoirs on Earth display a wide range of ^{12}C:^{13}C ratios. Typical $\delta^{13}C$ values for the major carbon reservoirs are illustrated in Figure 1. The importance of bond-breaking in creating a distinctly light (^{13}C-depleted) composition of organic matter is obvious, and the additional fermentation step during methanogenesis gives rise to ever more depleted methane carbon – i.e., there is a fractionation during photosynthesis and carbon assimilation as inorganic carbon is turned into organic molecules, and then a second stronger biological fractionation as organic matter is broken down and partly converted into CH_4.

Because the various reservoirs are characterized by different values of $\delta^{13}C$, moving carbon between from one to another will change not only the amount of carbon in the reservoirs but also potentially their $\delta^{13}C$. Repeated sampling of any one reservoir over time therefore enables input from (or loss to) a second reservoir to be inferred, even if changes in the size of either reservoir cannot be directly reconstructed. For instance, the isotopic composition of CO_2 in the atmosphere has declined from a pre-Industrial (ca. year 1800) value of about -6‰ to a present-day value of about -8.3 ‰,

reflecting the release of isotopically depleted fossil fuel carbon (ca. -27‰) to the atmosphere. Using this information together with a model representation of the exchange of carbon between atmosphere and ocean it is possible to reconstruct the expected history of atmospheric pCO_2 increases since the industrial revolution consistent with the observed $\delta^{13}C$ changes. In this particular example, measurements of historical atmospheric pCO_2 changes together with some information on the rate at which fossil fuel carbon has been burned and terrestrial biomass degraded are directly available and changes in pCO_2 do not have to be determined indirectly. However, in the absence of more direct measurements, $\delta^{13}C$ changes recorded in dated plant remains (the proxy) for example, combined with models, would have allowed us to reconstruct the history of atmospheric pCO_2 and the associated time-varying emissions of fossil fuel CO_2 to the atmosphere.

3.2. Reconstructing past steady-state modes of global carbon cycling

The geological record of carbon isotopic variability, illustrated in Figure 3, provides important insights into past carbon cycling. For the Phanerozoic (542 Ma to present; Figure 3a), the records are primarily derived from measurements made on the calcareous shells and skeletons of shallow dwelling and reef-forming organisms, supplemented by analyses on much smaller carbonate shells of planktic and benthic foraminifera for the interval for which ancient oceanic crust and its overlying sediment burden still exists (the last ~180 Myr). Organic matter may also help reconstruct $\delta^{13}C$ trends, although marine carbonates ($CaCO_3$) have the advantage of being much more abundant in sedimentary rocks than organic matter.

Overall, changes in the global carbon cycle through the Phanerozoic (Figure 3a) are reflected in relatively slow, multi-million year transitions between higher and lower $\delta^{13}C$. These intervals of elevated (or depleted) $\delta^{13}C$ can last 10s to 100s of Myrs and are generally ascribed to changes in the balance of organic vs. inorganic (carbonate) carbon burial. This is because the surficial carbon

348 reservoirs have insufficient capacity (Figure 1) to accumulate (or release) carbon at rates anywhere near
349 comparable to weathering or sediment burial (Figure 2) for such durations. Assuming steady state, i.e.
350 time scales much longer than the ca. 100 kyrs residence time of $\delta^{13}C$ in the modern surficial reservoirs,
351 the required mass balance can be written in terms of the ratio between organic carbon (F_{Corg}) and total
352 carbon ($F_{Corg} + F_{CaCO_3}$) burial fluxes:

353 $$\frac{F_{Corg}}{F_{Corg} + F_{CaCO_3}} = \frac{\delta^{13}C_{obs} - \delta^{13}C_{input}}{\Delta^{13}C_{Corg-CaCO_3}} \quad (2)$$

354 where $\delta^{13}C_{input}$ is the isotopic signature of the average carbon input into the ocean (Figure 1), and
355 $\Delta^{13}C_{Corg-CaCO_3}$ is the isotopic difference between the $\delta^{13}C$ of buried organic matter vs. that of $CaCO_3$.
356 (See e.g. *Kump and Arthur* [1999] for details.) Because the system is expressed as a function of the
357 observed $\delta^{13}C$ of the carbonate sediments ($\delta^{13}C_{obs}$), for approximately invariant rates of carbon inputs
358 and carbonate carbon burial ($F_{Corg} + F_{CaCO_3}$), Equation (2) reconstructs Earth's organic carbon burial
359 history from the observed $\delta^{13}C$ record (Figure 3). (One also needs to assume appropriate values for the
360 characteristic isotopic composition of carbon inputs and outputs ($\delta^{13}C_{input}$ and $\Delta^{13}C_{Corg-CaCO_3}$) as
361 summarized in Figure 2.) In other words: $\delta^{13}C_{obs}$ can be used as a proxy for the global burial rate of
362 organic matter, an important global carbon cycle flux that would otherwise be impossible to
363 reconstruct.

364 As an example, the increasing $\delta^{13}C_{obs}$ trend associated with the Carboniferous (359-299 Ma) in
365 Figure 3a is commonly interpreted as reflecting increasing organic matter burial in response to the
366 evolution of lignin-forming plants. Lignin is a relatively recalcitrant terrestrial compound that could
367 have caused a step increase in the efficiency of organic carbon preservation [*Berner*, 2004], for which
368 the extensive coal measures of the Carboniferous (a series of coal strata characteristic of the period) are

considered as supporting evidence. Proxies such as leaf stomata density suggest that atmospheric CO_2 declined to relatively low concentrations around this time [*Royer*, 2006] and a long interval of glaciation occurred – both consistent with an increase in organic carbon burial that sequestered CO_2 from the ocean and atmosphere. The important lesson here is that large observed changes in $\delta^{13}C$ may indicate fundamental reorganizations of the global carbon cycle.

3.3. Interpreting transient carbon cycle perturbations

Superimposed on the general underlying trends of gradually increasing and decreasing $\delta^{13}C$ are a wide variety of negative spikes and transients, illustrated in Figure 3c for the interval surrounding the Paleocene-Eocene boundary (ca. 56 Ma). Assuming that $\delta^{13}C$ transient changes reflect changes in the $\delta^{13}C$ of the seawater from which the carbonates are precipitated, rather than post-depositional diagenetic alteration, these negative spikes indicate that the relatively large ocean DIC and atmospheric CO_2 reservoirs are being contaminated by carbon with a distinct isotopic signature. In a simple mass balance approach, which deliberately ignores the fluxes into and out of the system unlike the approach above (Equation 2), we can write:

$$M_{final} \times \delta^{13}C_{M_{final}} \approx M_0 \times \delta^{13}C_{M_0} + \Delta M \times \delta^{13}C_{\Delta M} \quad (3a)$$

where the subscripts $_0$ and $_{final}$ represent the initial and final values of mass (M) and isotopic composition ($\delta^{13}C$) of the surficial carbon reservoir, and ΔM and $\delta^{13}C_{\Delta M}$ are the magnitude of the added carbon and its isotopic composition, respectively. Equation 3a simply states that the final mean isotopic composition of a carbon reservoir (here assumed to be surficial system of ocean + atmosphere + terrestrial biosphere + uppermost marine sediments) can be taken to be equal to the mean isotopic composition of the initial reservoir plus that of the added (or removed) carbon, all weighted by their respective masses. For a given isotopic signature of the new carbon, Equation 3a can be rearranged, substituting $M_{final} = M_0 + \Delta M$ (final carbon mass equals the initial mass plus carbon addition) and

392 $\delta^{13}C_{M_{final}} = \delta^{13}C_{M_0} + \Delta\delta^{13}C$ (final isotopic composition equals the initial isotopic composition plus the
393 recorded isotopic anomaly), to estimate the amount of carbon needed to explain a given magnitude of
394 isotopic excursion ($\Delta\delta^{13}C$):

395 $$\Delta M = -\Delta\delta^{13}C \times \frac{M_0}{\delta^{13}C_{M_0} + \Delta\delta^{13}C - \delta^{13}C_{\Delta M}} \quad (3b)$$

396 This relationship is illustrated in Figure 4 for assumed values of $\delta^{13}C_{M_0}$. An important caveat to this
397 analysis is that the carbon addition (or removal) is assumed to be instantaneous, i.e. that the excursion
398 is not significantly modified as a result of dilution caused by the continual throughput of carbon from
399 terrestrial weathering to marine sedimentation (Figure 2) whilst the new carbon is still being added (or
400 removed).

401 The transient event that occurs at the boundary between the Paleocene and Eocene Epochs
402 (Figure 3c) is a well-studied example of such a negative excursion event. The Paleocene (66-56 Ma)
403 and Eocene (56-33.9 Ma) are relatively warm intervals associated with elevated atmosphere pCO_2
404 compared to modern [*Hönisch et al.*, 2012] and a peak in warmth towards the early-middle Eocene
405 followed by a long-term cooling trend cumulating in the emergence of substantial ice on Antarctica in
406 the Oligocene (33.9-23.0 Ma). Tectonically, these intervals saw the movement of India towards and
407 then collision with the Asian plate and the disappearance of the remnant ancient Tethys Sea, together
408 with the gradual opening in the late Eocene and Oligocene of seaways separating Antarctica from
409 South America and Australia. The Paleocene-Eocene boundary itself is marked by a prominent
410 extinction amongst deep-sea foraminifera [*Thomas*, 2007] , being associated with a pronounced surface
411 warming characterized by a global mean temperature increase of about 5°C [*Dunkley Jones et al.*,
412 2013] – known as the Paleocene-Eocene Thermal Maximum ('PETM') [*Zachos et al.*, 2005].

413 A temporary negative shift in $\delta^{13}C$ associated with the PETM (Figure 3c) is recorded in all
414 superficial carbon reservoirs, from terrestrial wood, through marine algal compounds, to biogenic
415 carbonates [*McInerney and Wing*, 2011]. Because excursions for this event are recorded in a variety of
416 materials both on the land as well as in the ocean, we can be extremely confident that the $\delta^{13}C$ changes
417 are not simply a diagenetic artifact. The magnitude of the carbon isotope excursion does vary
418 somewhat amongst the different reservoirs, appearing amplified in organic matter closely connected to
419 the atmosphere and damped in biogenic carbonates deposited in deep marine sedimentary settings,
420 which complicates the interpretation [*Sluijs and Dickens*, 2012]. But assuming that the event's 'true'
421 value is around -4‰ for instance [*McInerney and Wing*, 2011; *Panchuk et al.*, 2008; *Sluijs and*
422 *Dickens*, 2012], one can estimate the amount of carbon released using Figure 4 (Eq. 4). The required
423 carbon release depends upon the specific $\delta^{13}C$ of the assumed source of carbon in this calculation.
424 Different sources of light carbon ranging from methane hydrates to deep ocean DOC and with different
425 characteristic $\delta^{13}C$ values have been suggested. Depending on the assumed carbon source and its
426 isotopic value, different amounts of carbon release would thus be inferred [*Panchuk et al.*, 2008]. This
427 is important information as knowing the amount of carbon released constrains the sensitivity of surface
428 temperatures to CO_2 increase, known as 'climate sensitivity' [*PALAEOSENS Project Members*, 2012].
429 For instance, a popular hypothesis is that destabilization of methane hydrates, with a characteristic $\delta^{13}C$
430 value of -60‰ (Figure 1), was central to the PETM event [*Dickens et al.*, 1995]. Assuming an initial
431 surficial carbon reservoir of ocean plus atmosphere plus terrestrial biosphere similar to modern
432 (~41,000 PgC (38,000 + 600 + 2000) – Figure 1) and an initial ocean $\delta^{13}C$ of 2‰ (Figure 3c), requires
433 a total carbon release from this source of 2,800 PgC for an excursion of -4‰. Alternatively, a terrestrial
434 organic carbon source at -22‰ [*Panchuk et al.*, 2008] such as might be derived from (burning) peat
435 deposits [*Kurtz et al.*, 2003] or oxidizing organic matter in Antarctic permafrost [*DeConto et al.*, 2012],
436 would require 8,200 PgC. An additional uncertainty is the assumed size of the past surficial carbon

reservoir. While we have some proxy constraints on atmospheric pCO_2 we have to rely on marine geochemical models in making hindcasts for the ocean DIC inventory (e.g. *Ridgwell* [2005]). Models suggest a similar-to-modern inventory for the Paleocene and Eocene [*Tyrrell and Zeebe*, 2004], though much further back in the past it could have been substantially larger [*Ridgwell*, 2005].

3.4. Ocean RDOC and ancient carbon cycling: An example from the Paleocene and Eocene

Difficulties arise in interpreting the PETM because the amounts of carbon estimated using Eq. 3b (and Figure 4) are often much larger than the size of the respective modern reservoirs (Figure 1). For a terrestrial carbon source of 8,200 PgC, the buildup of vast peat deposits during the late Paleocene, followed by a rapid oxidation in a 'global conflagration', would be required to explain the observations [*Kurtz et al.*, 2003]. For methane hydrates – the much warmer bottom water temperatures of the Paleocene and Eocene – 11°C in the deep ocean compared to ~2°C today [*Norris et al.*, 2013], would tend to substantially restrict the thickness and distribution of the hydrate stability zone and hence tend to decrease rather than increase the potential Paleocene hydrate reservoir [*Buffet and Archer*, 2004]. The controversial nature of these source scenarios has stimulated thinking about the potential role of DOC in ancient oceans.

Motivated partly by the apparent symmetry in the decline and recovery in $\delta^{13}C$ across some of the smaller apparent hyperthermal events that occurred subsequent to the PETM (Figure 3c), *Sexton et al.* [2011] suggested that changes in the ocean (refractory) DOC reservoir might have played a key role. Specifically, they proposed that fluctuations in the oxygenation of the Eocene ocean may have substantially altered the volume of anoxic waters and hence enabled RDOC to accumulate. Oxidizing this pool, perhaps as a consequence of changes in ocean circulation and hence oxygenation of deep waters, would drive a decline in $\delta^{13}C$ of marine carbonates. A subsequent replenishing of the reservoir would then drive the $\delta^{13}C$ of ocean DIC and hence carbonate carbon back to more positive values at the

460 end of the perturbation. These smaller isotopic fluctuations are characterized by $\delta^{13}C$ excursions of
461 only around -1‰ in magnitude compared to a PETM value of -4‰ and, therefore, require a smaller
462 carbon input. *Sexton et al.* [2011] estimated that a periodic accumulation and subsequent oxidation of
463 only ~1,600 PgC explains the observations – a value almost identical to a result from Eq. 4 assuming a
464 source isotopic signature of -25‰ (i.e. organic matter). An advantage of invoking ocean circulation
465 changes and associated variations in the ocean RDOC inventory is that it provides a mechanism that
466 explains why most of the hyperthermal events appear to be orbitally paced [*Lunt* et al., 2011]. (The
467 seasonal insolation received at high latitudes can differ sufficiently between different orbital
468 assumptions to drive large-scale changes in deep ocean ventilation in the South Atlantic in models –
469 see *Lunt* et al. [2011].)

470 Problems with the Paleogene hyperthermal DOC hypothesis primarily involve the (unknown)
471 sensitivity of RDOC degradation to ocean oxygenation. Assuming a modern production rate, an
472 approximate doubling of the (modern) inventory to ~1600 PgC would require a slow down of the
473 degradation rate to just under half its current rate. If in a simple Gedankenexperiment, one assumes that
474 the mean RDOC lifetime scales in inverse proportion to the oxic volume of the ocean, a doubling of the
475 RDOC lifetime requires a reduction of the oxic ocean volume to half of that today, i.e. each molecule
476 of RDOC would spend on average only half its time in oxygenated waters. Even these drastic
477 assumptions would only result in an isotopic excursion of <0.5‰ in magnitude. Yet there is no
478 evidence for such pervasive ocean anoxia developing during the Eocene. Even during peak warmth of
479 the PETM, only a few places in the deep ocean might have been anoxic [*Panchuk*, 2007]. Suggestions
480 that the deep ocean was not only anoxic but also stratified at depth [*Sexton et al.*, 2011] has the
481 advantage of creating an efficient deep ocean trap for RDOM, presumably generated deep in the water
482 column or released from the sediments, but falls foul of similar paleoceanographic observational
483 arguments against widespread seafloor anoxia. Also unanswered is the question of why the deep ocean

484 would become stratified and de-oxygenated prior to rather than during the transient warming and
485 associated negative $\delta^{13}C$ excursion.

486 *3.5. Ocean RDOC and ancient carbon cycling: An example from the Precambrian*

487 A more enigmatic feature of the geological record of global carbon cycling is the extreme variability in
488 $\delta^{13}C$ occurring during the Precambrian (prior to 541 Ma) (Figure 3b) and specifically during the
489 Neoproterozoic (541-1,000 Ma) (Figure 3d). The magnitude of this variation, with $\delta^{13}C$ reaching values
490 as low as -10 to -15‰, is much harder to explain from a reservoir change perspective using Eq. 3b than
491 is, for instance, the PETM. For example, prior to the evolution of land plants during the Ordovician
492 (488-444 Ma) there would have been little if any organic carbon stored on land, removing one potential
493 carbon source. This led Dan Rothman and colleagues [*Rothman et al.*, 2003] to identify isotopically
494 depleted oceanic DOC as a potentially key element in the Precambrian ocean. In their analysis, they
495 posited that a sufficiently large DOC reservoir would allow relatively small changes in DOC inventory
496 to exert a strong control on isotopic composition of oceanic DIC (+ atmospheric pCO_2) and hence the
497 measured $\delta^{13}C$ of marine carbonates. The absence of comparably extreme isotopic swings during the
498 Phanerozoic (Figure 3a) is ascribed to a 'terminal oxidation' event at the end of the Neoproterozoic
499 [*Rothman et al.*, 2003; *Swanson-Hysell et al.*, 2010] and the emergence of a modern mode of marine
500 carbon cycling characterized by a comparably small ocean DOC reservoir.

501 Building on this, *Peltier et al.* [2007] invoked oceanic DOC as part of a climate regulation
502 feedback that might have helped regulate climate and prevent run-away 'snowball' glaciation during
503 the Neoproterozic. Noting the temperature dependence of the solubility of oxygen in seawater, they
504 suggested that cooling ocean temperatures, in increasing the degree of oxygenation and hence
505 potentially the rate of oxidation of DOC, would have the effect of increasing atmospheric pCO_2 – a
506 negative and stabilizing feedback on climate cooling. Analogous inferences were drawn by *Swanson-*

507 *Hysell et al.* [2010] who proposed that the presence or absence of a massive oceanic DOC pool during
508 intervals of the late Neoproteroozic could have dictated the duration of the intervals between glaciation
509 via a strong negative feedback on cooling.

510 Whilst mathematically elegant, there are a number of difficulties with a DOC-dominant picture
511 of ancient carbon cycling and as an explanation for observed variations in carbonate $\delta^{13}C$. Firstly, we
512 lack direct or even indirect evidence for the existence of a massive pool of RDOC in the ocean.
513 Because in the *Rothman et al.* [2003] model this reservoir must be capable of buffering the isotopic
514 composition of the system, such a massive pool was assumed to have been at least 10 times the size of
515 the inorganic (ocean DIC + atmospheric pCO_2) reservoir. For a modern DIC + pCO_2 reservoir of
516 39,000 PgC, this equates to 390,000 PgC of DOC – more than 500 times larger than the modern
517 reservoir. There are reasons why the magnitude of the DIC + pCO_2 reservoir inventory might have
518 been still higher, hence requiring an even larger DOC inventory. For instance, model-based
519 reconstructions of long-term changes in ocean geochemistry suggest that at the beginning of the
520 Cambrian (542 Ma), the oceanic DIC reservoir could have been around 4 times its modern value (a
521 total of 152,000 PgC) [*Ridgwell*, 2005], with atmospheric pCO_2 as much as 20 times its modern value
522 [*Berner*, 2004]. This equates to a combined inorganic carbon reservoir of 164,000 PgC. The minimum
523 DOC reservoir then becomes 1.6×10^{6} PgC, equivalent to concentration of a little over 1000 mg DOC
524 per L of seawater (1.6×10^{21} gC in 1.4×10^{21} L of seawater) or ~0.07 mol kg^{-1}, which would make DOC
525 the third most dominant dissolved species in the ocean after Cl^- and Na^+. In comparison, even in the
526 Black Sea – a restricted basin that becomes anoxic below about 150 m water depth and receives large
527 dissolved organic matter loads via river input, observed DOC concentrations do not exceed 300 μmol
528 kg^{-1} (0.0003 mol kg^{-1}) (Ducklow et al., 2007).

529 Despite the extremely high oceanic DOC concentrations required, there is no obvious
530 mechanism or reasoning that precludes the build up of such a reservoir given many millions of years.

However, other considerations may help provide some (indirect) constraints on the dynamics of the ancient marine carbon cycle. The Shuram anomoly (Figure 3d), a feature occurring in multiple sections worldwide about 580 Ma and the largest carbon isotopic excursion in Earth history [*Fike et al.*, 2006; *Grotzinger et al.*, 2011], has been critically assessed in this context; i.e., whether DOC oxidation could be involved or whether other considerations place important constraints. The Shuram anomaly is characterized by a $\delta^{13}C$ minimum of -12‰ and a total duration estimated at some tens of millions of years [*Fike et al.*, 2006]. *Bristow and Kennedy* [2008] tackled the feasibility of a DOC-based explanation by considering whether an oxidant reservoir sufficient to convert DOC to DIC could have existed during the Neoproterozoic. Making plausible assumptions regarding late Neoproterozoic atmospheric oxygen and ocean sulphate concentrations, they generated a -12‰ excursion in a geochemical box model. However, the simulated excursion lasted ~0.5 Myr – some 1-2 orders of magnitude shorter than existing estimates for the event. It does not help to invoke a faster rate of O_2 production to help oxidize the DOC because O_2 is generally thought to be made available by the burial of organic matter, i.e. releasing oxygen associated with photosynthesis but preventing the organic matter produced from being re-oxidized. Burying more organic matter would also drive oceanic DIC $\delta^{13}C$ to be heavy as per Equation 2, opposing the influence of oxidized RDOC driving $\delta^{13}C$ lighter. These arguments can also be extended to glacial-associated negative anomalies occurring slightly earlier in the Neoproterozoic (Figure 3d). Hence, in the Precambrian, the much smaller than modern reservoirs of potential oxidants such as O_2 and SO_4^{2-} tend to argue against a dominant role for RDOC in accounting for large and particularly long-lived carbon isotopic excursions.

4. Implications for future global change?

As illustrated in Figure 3, Earth history contains a variety of perturbations of global climate and carbon cycling that are recorded in variations of geological proxies such as the carbon isotopic composition of sedimentary rocks. That many of these events have so far defied a simple or consensus explanation in terms of the source(s) of carbon behind the isotopic perturbation has stimulated interest in less 'conventional' carbon reservoirs and processes. If the reservoir size and cycling of carbon through DOC in the ancient oceans does play, at least at times, a key role in the Earth system and particularly in modulating atmospheric pCO_2, it is tempting to speculate how the modern DOC cycle might respond to on-going fossil fuel CO_2 emissions, with its attendant changes in climate. Of importance in the anthropogenic global change context is whether DOC might represent a positive (exacerbating) or negative (damping) feedback on atmospheric pCO_2 and climate. After all, there is sufficient RDOC in the ocean such that if it were to all be completely and instantaneously oxidized, it would deplete the global ocean dissolved oxygen inventory by about one third, driving substantial expansion of the intensity and extent of the oxygenation minimum zones of the ocean. Another view is that if all 630 PgC RDOC were to be oxidized to DIC and partitioned in the approximately 1:2 ratio characteristic of the equilibrium distribution of (fossil fuel) CO_2 between atmosphere and ocean [*Archer et al.*, 1997], it would represent a potential 100 ppm increase in atmospheric CO_2. (It should be noted that achieving such an equilibrium distribution takes several thousand years to achieve.)

There may be DOC removal/oxidation mechanisms that we have not yet appreciated and it is possible that the 630 PgC of RDOC residing in the ocean today is much more susceptible to rapid decay than its mean radiocarbon age would suggest. But is there really any evidence in the geological record that this is the case? We suggest that explaining the geological record of carbon isotopic excursions in terms of RDOC inventory changes need not necessarily require new and potentially

574 future-relevant mechanisms to be invoked. For instance, even for nominally rapid and abrupt
575 geological events such as the hyperthermals of the Paleocene and Eocene, the onset of the event may
576 have taken around 10 kyr [*McInerney and Wing,* 2011]. Taking a nominal lifetime (*e*-folding decay
577 time) of RDOC of 16 kyr [*Hansell*, 2013] implies that over an interval of 10 kyr, simply ceasing
578 production of RDOC at the start of the event would result in an approximate net CO_2 release of 300
579 PgC. For a marine DOC $\delta^{13}C$ source of ca. -25‰, this is sufficient, at steady state, to generate a -0.2‰
580 excursion in DIC $\delta^{13}C$ (Equation 3b, Figure 4). If prior to the PETM, a 20-fold larger than modern
581 RDOC inventory had accumulated, and again simply assuming that RDOC production ceases at the
582 onset of the event, one could obtain an excursion of about -4‰. Intermediate initial reservoir sizes
583 could be combined with additional inputs from the terrestrial biosphere, marine hydrates, and/or
584 enhanced volcanic out-gassing to achieve a -4‰ excursion overall. The net decay of such a RDOC
585 reservoir would in this example play its role as a positive feedback, responding to an initial
586 environmental change and amplifying it.

587 Although these are rather idealized and hypothetical scenarios, the point is that for negative
588 $\delta^{13}C$ excursions recorded in the geological record to at least partly reflect DOC dynamics, new or novel
589 removal/oxidation mechanisms are not needed *per se*. Instead, new mechanisms and understanding
590 about the controls on DOC generation may be necessary. Essentially, this is the hypothesis of
591 *Tziperman et al.* [2011], who invoked a decrease in the standing stocks of organic matter in the ocean
592 as the trigger of the $\delta^{13}C$ excursion associated with Neoproterozoic glaciation (Figure 3d). Their
593 assumed underlying driver was a biological innovation that led to the depletion of a pre-existing pool of
594 organic carbon in the ocean. Major evolutionary transitions cannot be invoked with the repeated
595 isotopic fluctuations during the Paleocene and Eocene and hence exact parallels cannot be drawn with
596 the Precambrian. However, biotic disruption is known to have occurred in association with some of the

larger events such as the PETM [*Hönisch et al.*, 2012; *Norris et al.*, 2013] and an interval of suppression of RDOC production and hence net organic matter oxidation is feasible.

In the context of understanding past events, we may also be focusing on the 'wrong' fraction of DOC. RDOC is an obvious candidate because the more labile fractions are rapidly degraded and in today's ocean comprise only a relatively small inventory – combined, only 20 PgC compared to the RDOC inventory of 630 PgC [*Hansell*, 2013]. It needs to be recognized that this is the situation for a well oxygenated modern ocean however. Analysis of the energetic potential from degrading different organic matter fractions [*LaRowe and Van Cappellen*, 2011] or lab incubations of sapropel organic matter [*Moodley et al.*, 2005] illustrates that a range of molecular structures such as membrane-type compounds that are degraded by bacteria in a well oxygenated ocean, may be rendered effectively refractory under anoxic conditions. These compounds, that today are classed as semi-refractory (SRDOC), might then accumulate in an anoxic (or euxinic) Precambrian ocean to create a massive DOC reservoir [*Ridgwell*, 2011]. In this scenario, RDOC concentrations need not change at all. Variations in the degree of anoxia could then induce large changes in the SRDOC rather than RDOC inventory but with similar implications for the interpretation of recorded $\delta^{13}C$ and global carbon cycling (and climate). An advantage of considering SRDOC in global carbon cycle dynamics is that it is produced at an order of magnitude faster rate than RDOC [*Hansell*, 2013].

The multi-millennial geological time scale of many past global carbon cycle and climate events and perturbations is well aligned, coincidently or not, with the long lifetime of RDOC. A promising way forward in this context would be to better understand the controls on and environmental sensitivities of production as well as consumption of RDOC today. Research into the fate of SRDOC in environments very different from those characterizing the modern ocean, perhaps the Black Sea, may also provide geologically-relevant insights. However, the extraordinary persistence in the ocean of the most refractory DOC fraction does not lend itself to providing any substantive future feedback with

621 future global change while the geological record has so far not provided any unambiguous evidence as
622 to whether oxidation and removal has ever been appreciably any faster or proved to be sensitive to
623 climate change.

624

625 ---

626

627 **Acknowledgements** AR and SA acknowledge support from The Royal Society in the form of University Research
628 Fellowship, and the Natural Environmental Research Council in the form of a Postdoctoral Fellowship, respectively.

629

630 ## References

631 Arndt, S., Jørgensen, B. B., LaRowe, D. E., Middelburg, J. J., Pancost, R. D., Regnier, P. Quantifying
632 the degradation of organic matter in marine sediments: A review and synthesis. Earth-Science
633 Reviews, 123, 53-86, 2013.

634 Arthur, M.A., Jenkyns, H.C., Brumsack, H.J., Schlanger, S.O. Stratigraphy, geochemistry and
635 paleoceanography of organic carbon-rich Cretaceous sequences, *in* Ginsburg R.N., Beaudoin B.,
636 eds., Cretaceous Resources, Events and Rhythms, NATO ASI Series, 1990.

637 Berner, R.A., The Phanerozoic Carbon Cycle: CO_2 and O_2, Oxford, Univ. Press, p. 160, 2004.

638 Biddanda, B. and Benner, R.. Carbon, nitrogen, and carbohydrate fluxes during the production of
639 particulate and dissolved organic matter by marine phytoplankton. Limnol. Oceanogr. 42, 506-518,
640 1997.

641 Bristow, T. and Kennedy, M.J. Carbon isotope excursions and the oxidant budget of the Ediacaran
642 atmosphere and ocean, Geology, 36, 863-866, 2008.

643 Buffett, B. and Archer, D. Global inventory of methane clathrate: sensitivity to changes in the deep
644 ocean, Earth and Planetary Science Letters 227, 185-199, 2004.

645 Cameron, D. R., Lenton, T. M., Ridgwell, A. J., Shepherd, J. G., Marsh, R., Yool, A. A factorial
646 analysis of the marine carbon cycle and ocean circulation controls on atmospheric CO_2, Global
647 Biogeochem. Cycles, 19, GB4027,doi:10.1029/2005GB002489, 2005.

Crill, P. M. and Martens, C. S. Biogeochemical cycling in an organic rich coastal marine basin: temporal and spatial variations in sulfate reduction rates. Geochimica et Cosmochimica Acta 51, 1175–1186, 1987.

DeConto, R. M., Galeotti, S., Pagani, M., Tracy, D., Schaefer, K., Zhang, T., Pollard, D., Beerling, D. J., Past extreme warming events linked to massive carbon release from thawing permafrost, Nature, 484(7392), 87–91, doi:10.1038/nature10929, 2012.

Dickens, G. R., O'Neil, J. R., Rea, D. K., Owen, R.M. Dissociation of oceanic methane hydrate as a cause of the carbon isotope excursion at the end of the Paleocene, Paleoceanography, 10, 965–971, doi:10.1029/95PA02087, 1995.

Ducklow, H. W., Quinby, H. L., Carlson, C. A. Bacterioplankton dynamics in the equatorial Pacific during the 1992 El Niño. Deep-Sea Res II 42, 621-638, 1995.

Ducklow, H. W., Hansell, D. A,. Morgan, J. A. Dissolved organic carbon and nitrogen in the Western Black Sea. Marine Chemistry 105, 140–150, 2007.

Dunkley-Jones, T., Lunt, D. L., Schmidt, D. N., Ridgwell, A., Sluijs, A., Valdes, P. J., Maslin, M. Climate model and proxy data constraints on ocean warming across the Paleocene-Eocene Thermal Maximum, Earth-Science Reviews, 125, 123-145, 2013.

Dunne, J., Sarmiento, J., and Gnanadesikan, A. A synthesis of global particle export from the surface ocean and cycling through the ocean interior and on the seafloor, Global Biogeochemical Cycles, 21, GB4006, doi:10.1029/2006GB002907, 2007.

667 Etheridge, D.M., Steele, L. P., Langenfelds, R. L., and Francey, R. J. Natural and anthropogenic
668 changes in atmospheric CO_2 over the last 1000 years from air in Arctic ice and firn. J. Geophys.
669 Res. 101, 4115-28, 1996.

670 Feely, R. A., Sabine, C. L., Lee, K., Berelson, W., Kleypas, J., Fabry, V. J., Millero, F. J.,Impact of
671 anthropogenic CO_2 on the $CaCO_3$ system in the oceans, Science, 305, 362– 366, 2004.

672 Fike, D.A., Grotzinger, J.P., Pratt, L.M., Summons, R.E. Oxidation of the Ediacaran Ocean: Nature,
673 444, 744–747, doi: 10.1038/nature05345, 2006.

674 Gibbs, S. J., Bralower, T. J., Bown, P. R., Zachos, J. C., Bybell, L. Shelf and open-ocean calcareous
675 phytoplankton assemblages across the Paleocene-Eocene Thermal Maximum: Implications for
676 global productivity gradients, Geology, 34, 233–236, 2006.

677 Gibbs, S. J., Bown, P. R., Murphy, B. H., Sluijs, A., Edgar, K. M., Pälike, H., Bolton, C. T., Zachos, J.
678 C. Scaled biotic disruption during early Eocene global warming events. Biogeosciences, 9, 4679-
679 4688, 2012.

680 Grotzinger, J., Fike, D., Fischer, W.. Enigmatic origin of the largest known carbon isotope excursion in
681 Earth's history. Nat. Geoscience, 4, 285–292, 2011.

682 Hain, M.P., Sigman, D.M., and Haug, G.H. The Biological Pump in the Past, in Treatise on
683 Geochemistry, Second Edition, vol.6, ed. Mottl M.J., and Elderfield, H., in press.

684 Hansell, D. Recalcitrant Dissolved Organic Carbon Fractions. Annual Review of Marine Science, 5,
685 pp. 421-445, 2013.

686 Halverson, G. P., Hoffman, P. F., Schrag, D. P., Maloof, A. C., Hugh, A., Rice, N., Toward a
687 Neoproterozoic composite carbon-isotope record. GSA Bulletin 117, 1181–1207; doi:
688 10.1130/B25630.1, 2005.

689 Hönisch, B., Ridgwell, A., Schmidt, D. N., Thomas, E., Gibbs, S. J., Sluijs, A., Zeebe, R. E., Kump,
690 L., Martindale, R. C., Greene, S. E., Kiessling, W., Ries, J., Zachos, J., Royer, D. L., Barker, S.,
691 Marchitto Jr., T. M., Moyer, R., Pelejero, C., Ziveri, P., Foster G. L., Williams, B. The Geological
692 Record of Ocean Acidification, Science, Volume 335, 1058-1063, 2012.

693 IPCC AR4 WG1, Solomon, S.; Qin, D.; Manning, M.; Chen, Z.; Marquis, M.; Averyt, K.B.; Tignor,
694 M.; and Miller, H.L., ed., Climate Change 2007: The Physical Science Basis, Contribution of
695 Working Group I to the Fourth Assessment Report of the Intergovernmental Panel on Climate
696 Change, Cambridge University Press, ISBN 978-0-521-88009-1, 2007.

697 Jiao, N., Herndl, G. J., Hansell, D. A., Benner, R., Kattner, G., Wilhelm, S. W., Kirchman, D. L.,
698 Weinbauer, M. G., Luo, T., Luo, T., and Chen, F. Microbial production of recalcitrant dissolved
699 organic matter: long-term carbon storage in the global ocean. Nature Rev. Microbiol. 8, 593–599,
700 2010.

701 Jiao N., Azam F., Sanders S., (eds). Microbial carbon pump in the ocean. Science/AAAS, Washington
702 DC: doi:10.1126/science.opms.sb0001, 2011.

703 Jørgensen, B. B., Sørensen, J. Seasonal cycles of O_2, NO_3^- and SO_4^{2-} reduction in estuarine sediments:
704 the significance of a nitrate reduction maximum in spring. Marine Ecology Progress Series 24, 65–7,
705 1985.

706 Keeling R.F., Körtzinger A., Gruber N. Ocean deoxygenation in a warming world: Annual Review of
707 Marine Science, 2, 199–229,doi:10.1146/annurev.marine.010908.163855, 2010.

708 Kohfeld, K. E. and Ridgwell, A. Glacial-interglacial variability in atmospheric CO_2, in: Surface
709 Ocean/Lower Atmosphere Processes, Geophysical Monograph Series 37, edited by: Le Quere, C.
710 and Saltzman, E., American Geophysical Union, Washington, DC, 2009.

711 Kump, L.R. and Arthur, M.A. Interpreting carbon-isotope excursions: carbonates and organic matter.
712 Chemical Geology 161, 181-198, 1999.

713 Kurtz, A., Kump, L., Arthur, M., Zachos, J., Paytan, A. Early Cenozoic decoupling of the global carbon
714 and sulfur cycles. Paleoceanography 18, 1090, 2003.

715 Lambert, F., Bigler, M., Steffensen, J. P., Hutterli, M., Fischer, H. Centenial mineral dust variability in
716 high-resolution ice core data from Dome C, Antarctica. Clim. Past, 8, 609-623, 2012.

717 LaRowe D. E., and Van Cappellen, P. Degradation of natural organic matter: A thermodynamic
718 analysis. Geochim Cosmochim Acta 75, 2030–2042, 2011.

719 Lorius, C., Jouzel, J., Raynaud, D. The ice core record: past archive of the climate and signpost to the
720 future. In: Antarctica and Environmental Change. Oxford Science Publications. 27-34. 1993.

721 Lunt, D., Ridgwell, A., Sluijs, A., Zachos, J., Hunter, S., Haywood, A. A model for orbital pacing of
722 methane hydrate destabilization during the Palaeogene. Nature Geoscience, 4, 775 – 778, 2011.

723 Maslin, M.A., and Thomas, E. Balancing the deglacial global carbon budget: the hydrate factor. QSR,
724 15-17, 1729-1736, 2003.

725 Maslin, M., Owen, M., Betts, R., Day, S., Dunkley Jones, T. Ridgwell, A. Gas hydrates: past and future
726 geohazard?, Phil. Trans. R. Soc. A 368, 2369-2393, doi:10.1098/rsta.2010.0065, 2010.

727 Matsumoto, K., Hashioka, T., Yamanaka, Y. Effect of temperature-dependent organic carbon decay on
728 atmospheric pCO2, J. Geophys. Res., 112, G02007, doi:10.1029/2006JG000187, 2007.

729 McInerney, F.A. and Wing, S.L. The Paleocene-Eocene Thermal Maximum: A perturbation of carbon
730 cycle, climate, and biosphere with implications for the future. Annual Review of Earth and Planetary
731 Sciences 39, 489-516, 2011.

732 Monnin, E., Indermühle, A. Dällenbach, A., Flückiger, J., Stauffer, B., Stocker, T. F., Raynaud, D.,
733 Narnola, J.-M. Atmospheric CO_2 Concentrations over the Last Glacial Termination. Science. 291,
734 112-114, 2001.

735 Moodley, L., Middelburg, J.J. Herman, P.M.J., Soetaert, K. de Lange, G.J. Oxygenation and organic
736 matter preservation in marine sediments: Direct experimental evidence from ancient organic carbon-
737 rich deposits. Geology, 33, 889-892, 2005.

738 Norris, R. D., Kirtland Turner, S., Hull, P. M., Ridgwell, A. Marine ecosystem responses to Cenozoic
739 global change, Science, 341, 492-498, 2013.

740 Panchuk, K. Investigating the Paleocene/Eocene Carbon Cycle Perturbation: An Earth System Model
741 Approach, Ph.D. Dissertation, The Pennsylvania State University, 2007.

742 Panchuk, K., Ridgwell, A., Kump, L. R. Sedimentary response to Paleocene Eocene Thermal
743 Maximum carbon release: A model-data comparison, Geology 36, 315-318, 2008.

744 Peltier, R.W., Liu, Y., Crowley, J. W. Snowball Earth prevention by dissolved organic carbon
745 remineralization. Nature, 450, 813-818, 2007.

746 Ridgwell, A. J., Kennedy, M. J., Caldeira, K. Carbonate deposition, climate stability, and
747 Neoproterozoic ice ages, Science, 302, 859-862, 2003.

748 Ridgwell, A. A Mid Mesozoic revolution in the regulation of ocean chemistry. Marine Geology, 217,
749 339-357, 2005.

750 Ridgwell, A., and Schmidt, D. N. Past constraints on the vulnerability of marine calcifiers to massive
751 CO2 release, Nature Goescience, doi:10.1038/ngeo755, 2010.

752 Ridgwell, A., Evolution of the ocean's "biological pump", PNAS 108, 16485–16486, 2011.

753 Rohling, E.J., Sluijs, A., Dijkstra, H. A., Köhler, P., van de Wal, R.S.W., von der Heydt, A.S.,
754 Beerling, D.J., Berger, A., Bijl, P.K., Crucifix, M., DeConto, R., Drijfhout, S. S., Fedorov, A.,
755 Foster, G. L., Ganopolski, A., Hansen, J., Hönisch, B., Hooghiemstra, H., Huber, M., Huybers, P.,
756 Knutti, R., Lea, D. W., Lourens, L. J., Lunt, D., Masson-Demotte, V., Medina-Elizalde, M., Otto-
757 Bliesner, O., Pagani, M., Pälike, H., Renssen, H., Royer, D. L., Siddall, M., Valdes, P., Zachos, J.
758 C., Zeebe, R. E. Making sense of palaeoclimate sensitivity, Nature, 491, 683-691, 2012.

759 Rothman, D.H., Hayes, J.M.., Summons, R.E. Dynamics of the Neoproterozoic carbon cycle.
760 Proceedings of the National Academy of Sciences USA 100, 8124-8129, 2003.

761 Royer, D. L. Stomatal density and stomatal index as indicators of paleoatmospheric CO_2 concentration.
762 Review of Palaeobotany and Palynology, 114, 2001.

763 Royer, D. L., CO_2-forced climate thresholds during the Phanerozoic, Geochimica et Cosmochimica
764 Acta 70, 5665–5675, 2006.

765 Sarmiento, J. L. and Gruber. N. Ocean Biogeochemical Dynamics, Princeton University Press,
766 Princeton, NJ, 526, 2006.

767 Sexton, P.F., Norris, R.D., Wilson, P.A., Pälike, H., Westerhold, T., Röhl, U., Bolton, C., Gibbs, S.
768 Eocene global warming events driven by ventilation of oceanic dissolved organic carbon, Nature,
769 471, 349-352, doi:10.1038/nature09826, 2011.

770 Shields, G., and Veizer, J., Precambrian marine carbonate isotope database: version 1.1. Geochemistry
771 Geophysics Geosystems 3, 108- 113, 2002.

772 Sluijs, A., and Dickens, G. R. Assessing offsets between the $\delta^{13}C$ of sedimentary components and the
773 global exogenic carbon pool across early Paleogene carbon cycle perturbations, Global
774 Biogeochemical Cycles, 26, DOI: 10.1029/2011GB004224, 2012.

775 Stumm, W. and Morgan, J. J. Aquatic Chemistry, 2n Ed. New York: Wiley-Interscience. pp. 780, 1981.

776 Swanson-Hysell, N.L., Rose, C.V., Calmet, C.C., Halverson, G.P., Hurtgen, M.T., Maloof, A.C.
777 Cryogenian glaciation and the onset of carbon-isotope decoupling. Science, 328, 608-611,
778 doi:10.1126/science.1184508, 2010.

779 Tyrrell, T., and Zeebe, R. E. History of carbonate ion concentration over the last 100 million years,
780 Geochimica et Cosmochimica Acta, 68, 3521–3530, 2004.

781 Tziperman, E., Halevy, I., Johnston, D. T., Knoll, A. H., Schrag, D. P. Biologically induced initiation
782 of Neoproterozoic snowball-Earth events. Proc Natl Acad Sci USA 108, 15091–15096, 2011.

783 Watson, R. T., Noble, I. R., Bolin, B., Ravindramath, N. H., Verardo, D. J., Dokken D. J, (eds). Land
784 Use, Land-Use Change, and Forestry (a special Report of the IPCC). Cambridge University Press,
785 Cambridge, pp. 377, 2000.

786 Wefer, G., Berger, W. H., Bijma, J., Fischer, G. Clues to ocean history: A brief overview of proxies, in:
787 G. Fischer, G. Wefer (Eds.), Use of Proxies in Paleoceanography: Examples from the South
788 Atlantic, Springer, Berlin, pp. 1-68, 1999.

789 Zachos, J. C., McCarren, H., Murphy, B., Rohl, U., Westerhold, T. Tempo and scale of late Paleocene
790 and early Eocene carbon isotope cycles: Implications for the origin of hyperthermals. Earth Planet.
791 Sci. Lett. 299, 242-249, 2010.

792 Zeebe, R. E. and Wolf-Gladrow, D.. CO_2 in Seawater: Equilibrium, Kinetics, Isotopes. Elsevier
793 Oceanography Series, Amsterdem, 65, pp. 346, 2001.

794
795

796

Figure 1.

Illustration of the primary reservoirs and processes constituting the (natural) global carbon cycle. Approximate carbon inventories (brackets) and representative carbon isotopic compositions (blue and in parentheses) are shown for the main reservoirs and fluxes. Adapted from *Hönisch et al.* [2012] with representative isotopic compositions from *Maslin and Thomas* [2003] and inventories from *IPCC* [2007].

Figure 2.

Schematic workings of the four components of the ocean's carbon pump.

Panel A illustrates the solubility pump, with CO_2 taken up by the ocean predominantly in cold surface waters, transported via ocean circulation, and eventually up-welled/mixed to the warmer surface waters where CO_2 is returned to the atmosphere.

Panel B illustrates the particulate organic carbon pump in the ocean.

Panel C illustrates the carbonate pump in the ocean.

Panel D illustrates the cycle of dissolved organic carbon in the ocean and the microbial carbon pump. Fluxes of DOC are broken down into semi-labile (light grey) and semi-refractory (dark grey), neither of which are transported far into the ocean interior. Fluxes of refractory DOC (RDOC) are indicated with black arrows. Reservoir inventories, in brackets, are from *Hansell* [2013].

In all panels: carbon fluxes into the ocean are shown in normal font, and sinks in italics. For panels A-C, these are quantified following *Hönisch et al.* [2012] in units of PgC yr^{-1}.

Figure 3.

Carbon isotopic variability through Earth history. Shown are compilations of $\delta^{13}C$ measured in marine carbonates for the Phanerozoic in panel A [*Veizer et al.*, 1999] and for the Precambrian in panel B [*Shields et al.*, 2002]. Panel C shows a more detailed benthic foraminiferal calcite $\delta^{13}C$ record spanning the Paleocene-Eocene boundary [*Zachos et al.*, 2010]. The timing of hyperthermal events are indicated by red triangles. Panel D shows a more detailed record spanning the mid through late Neoproterozoic [*Halverson et al.*, 2005; *Macdondald et al.* (2012)]. The approximate age of occurrence of glaciations

823 are marked with inverted blue triangles. In the geological time scale at the top, the abbreviated Periods,
824 from left to right are: Neogene ('Ng'), Paleogene ('Pg'), Cretaceous ('K'), Jurassic ('J'), Triassic ('T'),
825 Permian ('P'), Carboniferous ('C'), Devonian ('D'), Silurian ('S'), Ordovician ('O'), and Cambrian
826 ('Cm').

827 **Figure 4.**

828 The relationship between carbon source size, isotopic signature, and resulting excursion magnitude.
829 Contours delineating the relationship between source magnitude and isotopic composition for a -4‰
830 carbon isotopic ($\delta^{13}C$) composition as given by Eq. 4. The assumed $\delta^{13}C$ of the carbon source is on the
831 x-axis, with the resulting inferred mass of carbon (in PgC) on the y-axis. Contours are plotted for initial
832 mean surficial carbon reservoir $\delta^{13}C$ values spanning the observed range of long-term Phaneroozic
833 variability: -2‰ (pink), 0‰ (orange), 2‰ (green), 4‰ (light blue), and 6‰ (dark blue).

834

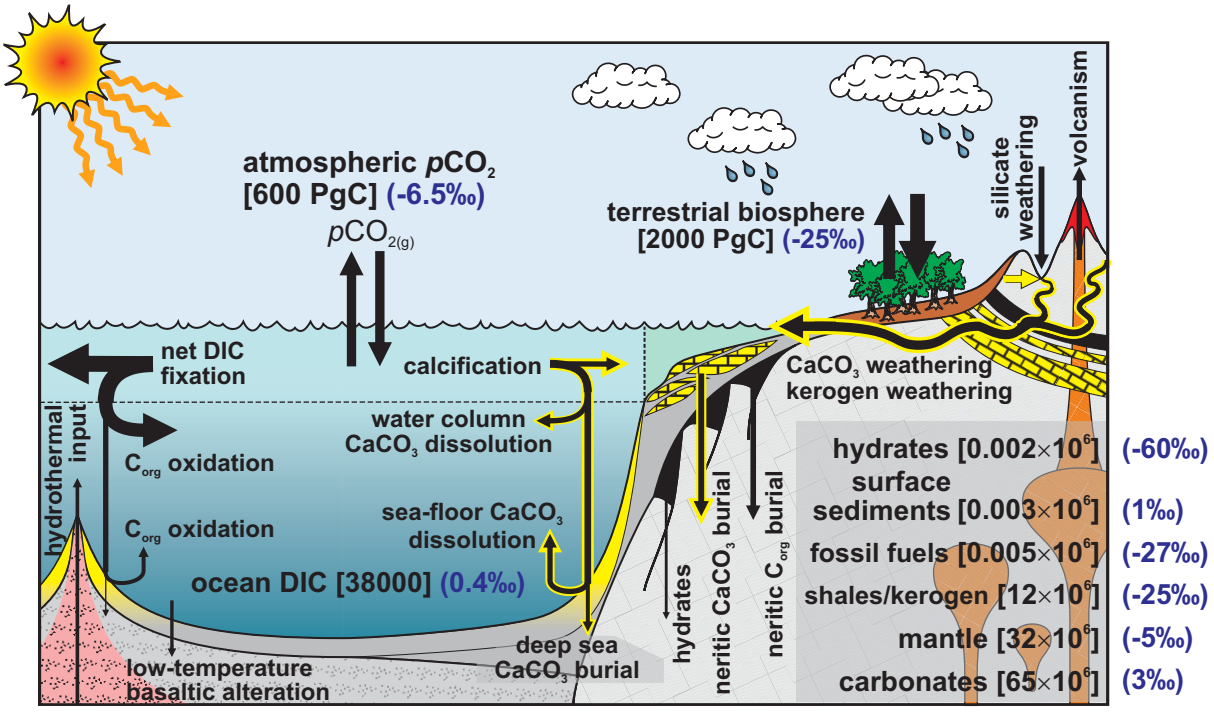
atmospheric pCO2
[600 PgC] (-6.5‰)
pCO2(g)
terrestrial biosphere
[2000 PgC] (-25‰)
silicate weathering
volcanism
net DIC fixation
calcification
CaCO3 weathering
kerogen weathering
water column
CaCO3 dissolution
hydrothermal input
Corg oxidation
Corg oxidation
sea-floor CaCO3 dissolution
ocean DIC [38000] (0.4‰)
hydrates
neritic CaCO3 burial
neritic Corg burial
deep sea
CaCO3 burial
low-temperature
basaltic alteration
hydrates [0.002×10^6] (-60‰)
surface sediments [0.003×10^6] (1‰)
fossil fuels [0.005×10^6] (-27‰)
shales/kerogen [12×10^6] (-25‰)
mantle [32×10^6] (-5‰)
carbonates [65×10^6] (3‰)

Figure 1

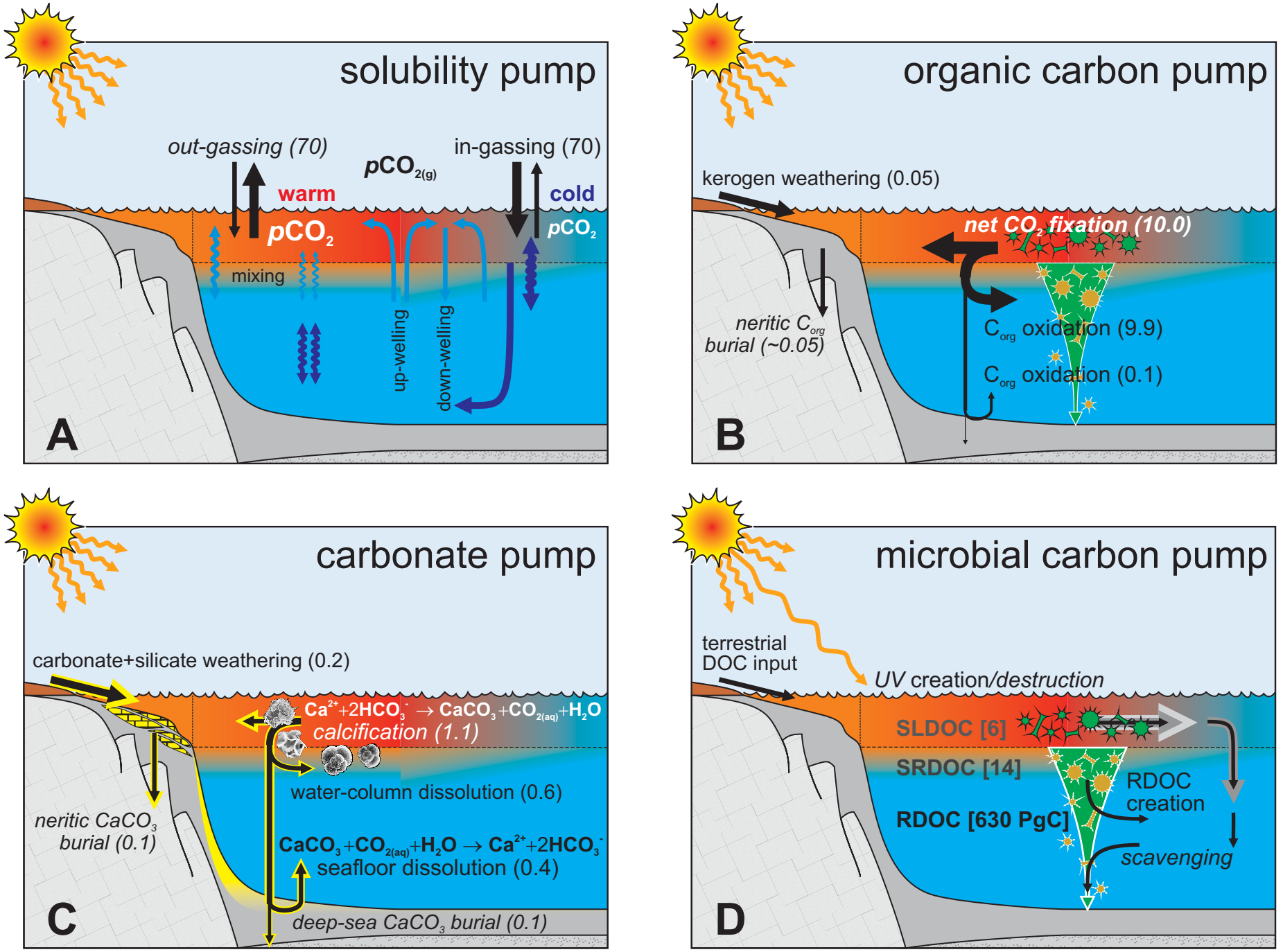
solubility pump
out-gassing (70)
in-gassing (70)
pCO2(g)
warm
cold
pCO2
pCO2
mixing
up-welling
down-welling
A
organic carbon pump
kerogen weathering (0.05)
net CO2 fixation (10.0)
neritic Corg burial (~0.05)
Corg oxidation (9.9)
Corg oxidation (0.1)
B
carbonate pump
carbonate+silicate weathering (0.2)
Ca2+ +2HCO3- → CaCO3 +CO2(aq) +H2O
calcification (1.1)
water-column dissolution (0.6)
neritic CaCO3 burial (0.1)
CaCO3 +CO2(aq) +H2O → Ca2+ +2HCO3-
seafloor dissolution (0.4)
deep-sea CaCO3 burial (0.1)
C
microbial carbon pump
terrestrial DOC input
UV creation/destruction
SLDOC [6]
SRDOC [14]
RDOC [630 PgC]
RDOC creation
scavenging
D

Figure 2

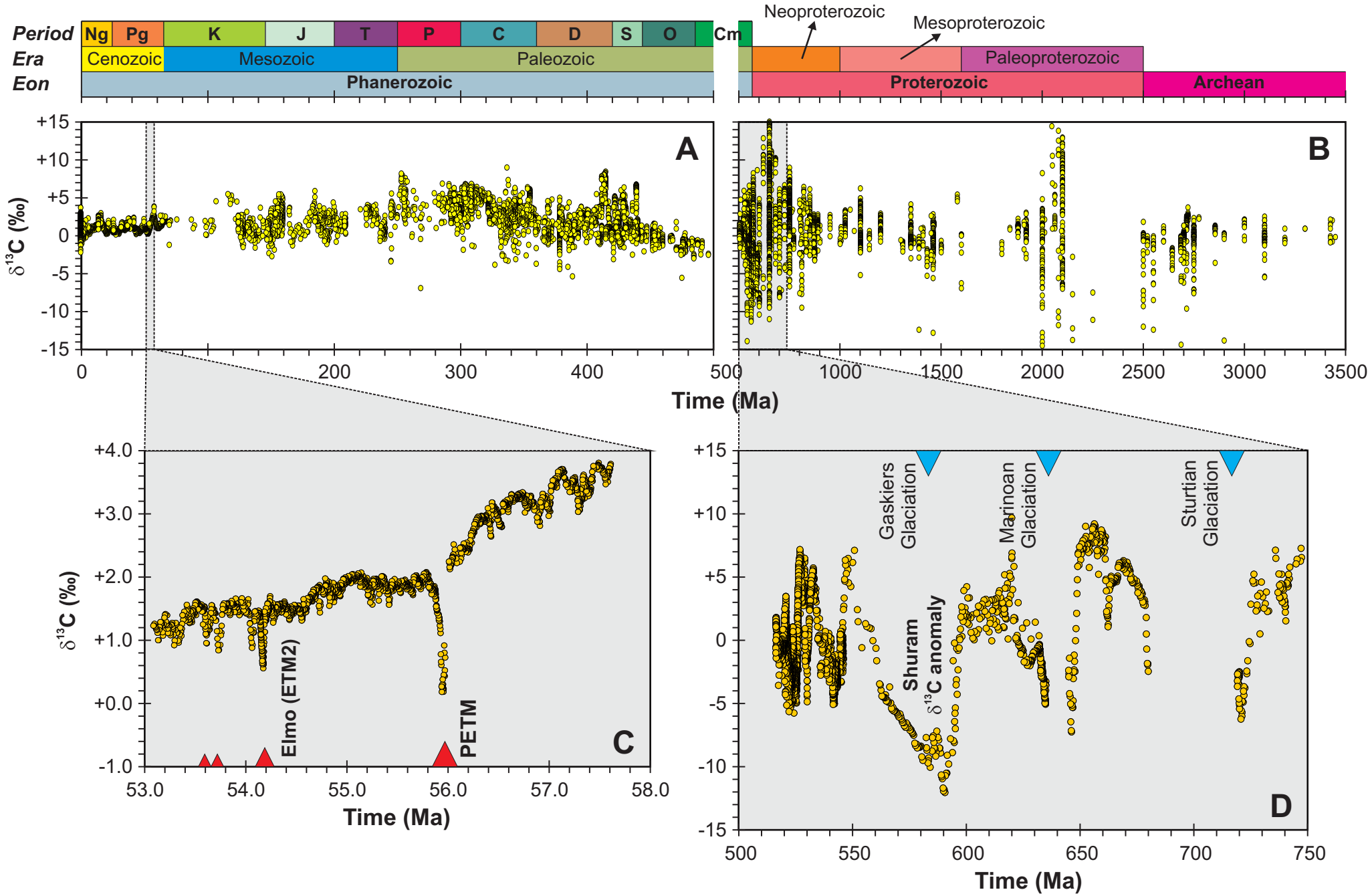
Period
Era
Eon
Ng
Pg
K
J
T
P
C
D
S
O
Cm
Cenozoic
Mesozoic
Paleozoic
Phanerozoic
Neoproterozoic
Mesoproterozoic
Paleoproterozoic
Proterozoic
Archean
A
B
C
D
δ13C (‰)
Time (Ma)
Elmo (ETM2)
PETM
Gaskiers Glaciation
Marinoan Glaciation
Sturtian Glaciation
Shuram δ13C anomaly

Figure 3

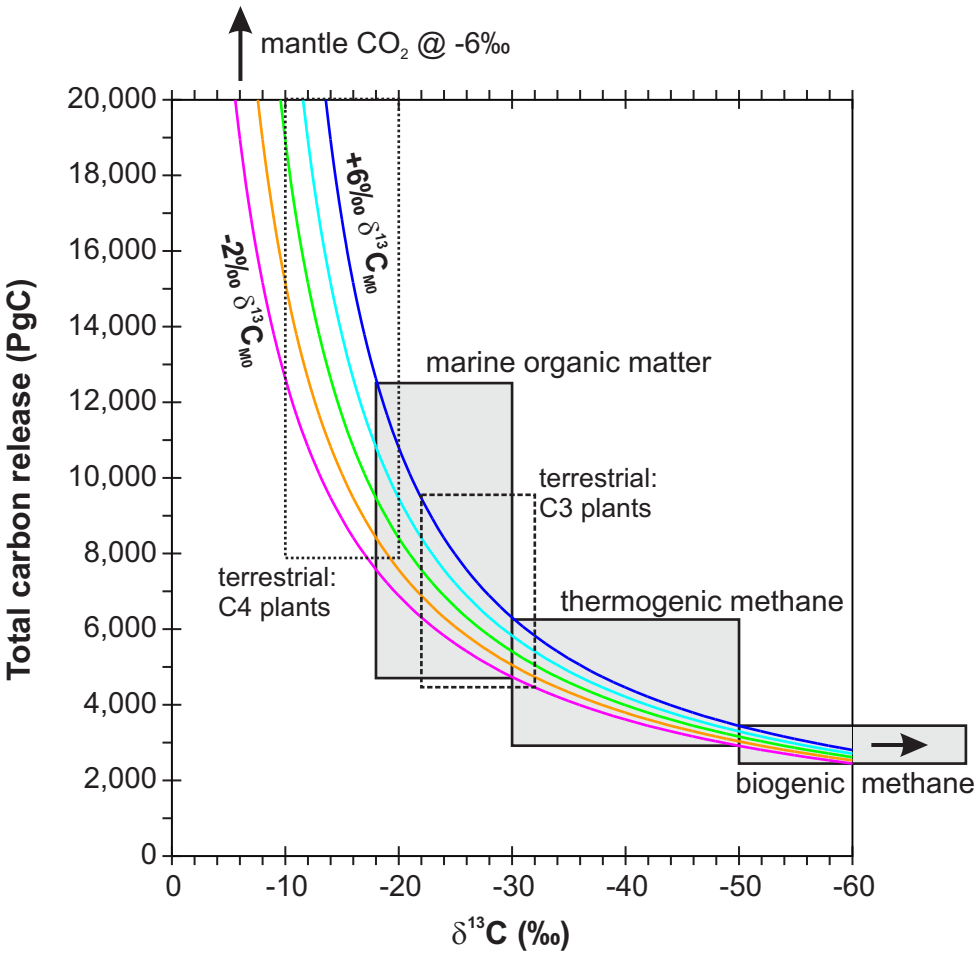
mantle CO2 @ -6‰
20,000
18,000
16,000
14,000
12,000
10,000
8,000
6,000
4,000
2,000
0
Total carbon release (PgC)
+6‰ δ13CM0
-2‰ δ13CM0
marine organic matter
terrestrial:
C3 plants
terrestrial:
C4 plants
thermogenic methane
biogenic methane
0
-10
-20
-30
-40
-50
-60
δ13C (‰)

Figure 4